

Looking for age-related growth decline in natural forests: unexpected biomass patterns from tree rings and simulated mortality

Jane R. Foster · Anthony W. D'Amato ·
John B. Bradford

Received: 9 May 2013 / Accepted: 3 January 2014 / Published online: 18 January 2014
© Springer-Verlag Berlin Heidelberg 2014

Abstract Forest biomass growth is almost universally assumed to peak early in stand development, near canopy closure, after which it will plateau or decline. The chronosequence and plot remeasurement approaches used to establish the decline pattern suffer from limitations and coarse temporal detail. We combined annual tree ring measurements and mortality models to address two questions: first, how do assumptions about tree growth and mortality influence reconstructions of biomass growth? Second, under what circumstances does biomass production follow the model that peaks early, then declines? We integrated three stochastic mortality models with a census tree-ring data set from eight temperate forest types to reconstruct stand-level biomass increments (in Minnesota, USA). We compared growth patterns among mortality models, forest types and stands. Timing of peak biomass growth varied significantly among mortality models, peaking 20–30 years earlier when mortality was random with respect to tree

growth and size, than when mortality favored slow-growing individuals. Random or u-shaped mortality (highest in small or large trees) produced peak growth 25–30 % higher than the surviving tree sample alone. Growth trends for even-aged, monospecific *Pinus banksiana* or *Acer saccharum* forests were similar to the early peak and decline expectation. However, we observed continually increasing biomass growth in older, low-productivity forests of *Quercus rubra*, *Fraxinus nigra*, and *Thuja occidentalis*. Tree-ring reconstructions estimated annual changes in live biomass growth and identified more diverse development patterns than previous methods. These detailed, long-term patterns of biomass development are crucial for detecting recent growth responses to global change and modeling future forest dynamics.

Keywords Stand dynamics · Dendrochronology · Net primary productivity · Temperate forests · Sub-boreal forests

Communicated by Ram Oren.

Electronic supplementary material The online version of this article (doi:10.1007/s00442-014-2881-2) contains supplementary material, which is available to authorized users.

J. R. Foster (✉) · A. W. D'Amato
Department of Forest Resources, University of Minnesota, 115
Green Hall, 1530 Cleveland Avenue N, St Paul, MN 55108, USA
e-mail: jrfooster@umn.edu

A. W. D'Amato
e-mail: damato@umn.edu

J. B. Bradford
U.S. Geological Survey, Southwest Biological Science Center,
Colorado Plateau Research Station, Northern Arizona University,
Building 56, P.O. Box 5614, Flagstaff, AZ 86011, USA
e-mail: jbradford@usgs.gov

Introduction

Production of woody biomass changes as forest trees and stands age. How productivity changes with age is critical to models of forest yield and C dynamics. Though many such models exist, their applicability across natural systems remains uncertain (Wirth 2009). Conventional wisdom holds that aggregate woody biomass growth will increase rapidly following stand initiation, peak at or shortly after canopy closure, then decline to a constant or decreasing rate of biomass production (Bormann and Likens 1979; Gower et al. 1996; Ryan et al. 1997, 2004; Caspersen et al. 2000; Smith and Long 2001). The most prevalent explanations for this pattern hypothesize that biomass increments

diminish as stands age as a result of declining net primary productivity (NPP) (Ryan et al. 2004), increasing mortality (Coomes et al. 2012; Xu et al. 2012), or some combination of both processes (Acker et al. 2002; Wirth 2009). Previous studies have tested aspects of these hypotheses observationally and experimentally, often using fast-growing plantations or even-aged, monospecific forest types as study systems, with varied results (Binkley et al. 2002; Ryan et al. 2004; Coomes et al. 2012).

While a decline in biomass increment has been documented for many aging forest stands (Pregitzer and Euskirchen 2004), recent findings in old-growth forests question the prevalence of this pattern (Luyssaert et al. 2008; Lichstein et al. 2009; Rhemtulla et al. 2009). Moreover, individual trees can increase wood production over their natural life span (Phipps and Whiton 1988; Duchesne et al. 2003; Johnson and Abrams 2009). This evidence needs to be reconciled with stand-level models of wood production, particularly as the assumed pattern of age-related decline is currently propagating through a new generation of data- and theory-driven models of forest growth (Caspersen et al. 2011; Coomes et al. 2012). To ensure that models are realistic and broadly applicable, there is a need for empirical assessments of the peaked model of biomass production in a wider range of natural forests (Bradford and Kastendick 2010).

Aboveground biomass increment is measured as the change in aggregate woody biomass between two points in time. It is a major component of NPP that is most frequently estimated from field measurements (Clark et al. 2001; Davis et al. 2009), typically by applying allometric regression equations to tree diameter data from repeat forest inventories or less often from dendrochronological reconstructions. Because forests develop slowly (over decades or centuries), and can span a complex range of species and structural mixes, direct measurements of the pools or fluxes constituting rates of aboveground biomass change are generally sparse and incomplete in either the temporal or spatial domain (Clark et al. 2001, 2007). Chronosequences are often employed to infer temporal patterns of biomass change from current conditions, but suffer from limitations due to imperfect substitutions of space for time (Johnson and Miyanishi 2008). As a consequence of the coarse temporal resolution typical of chronosequence or repeat inventory methods used to measure biomass change (often decadal time steps or greater), our understanding of temporal details is incomplete.

These shortcomings can be partially overcome by the use of dendrochronological data, which provide an annually resolved and lengthy reconstruction of wood production through forest stand development. However, tree-ring records from live-tree censuses underestimate past biomass increments because they do not account for growth

of trees that died before the census (Clark et al. 2001). We cannot accurately evaluate temporal patterns in stand biomass increment without accounting for the growth of these dead trees (Malhi et al. 2004). Yet many studies that compare current to past growth rates in order to assess effects of phenomena such as rising atmospheric CO₂ levels and possible fertilization (Cole et al. 2010) or climatic variation associated with global change (Williams et al. 2010) largely ignore growth lost to past mortality or other demographic processes, possibly contributing to biased conclusions (Foster et al. 2010; Brienen et al. 2012). Ecologists need valid methods to account for growth lost to past mortality for reliable comparison, reconstruction and modeling of stand-level growth rates over time (Caspersen et al. 2000; Foster et al. 2010).

To address this need, we estimated past mortality and growth by linking tree-ring data with a retrospective simulation approach. We integrated three mortality models with a census tree-ring data set from eight temperate forest communities to assess stand biomass increment patterns. First, we asked: how do assumptions about individual-tree mortality influence long-term estimates of stand-level biomass increment (i.e., growth)? Specifically, we determined how the estimated timing and magnitude of peak growth varied when assuming different models of probabilistic mortality, or different definitions of growth (i.e., live vs. net biomass increment). Second, we used the long-term estimates of total growth that included simulated mortality to ask: under what circumstances does woody biomass production of naturally established forests follow the assumed model of growth that peaks early in stand development? Specifically, we identified stand structural and compositional characteristics that were related to biomass development patterns, and asked whether patterns were consistent with existing evidence of stand growth and optimization in forests of varying developmental stages and species mixes (Smith and Long 2001; Binkley et al. 2002; Metsaranta and Lieffers 2010; Coomes et al. 2012; Xu et al. 2012).

Materials and methods

Study area

The Superior National Forest (SNF) in northern Minnesota, USA (Fig. 1) falls in a latitudinal transition zone between temperate forests to the south and boreal forest ecosystems to the north. A significant national wilderness reserve, the Boundary Waters Canoe Area Wilderness, lies just north of the SNF and is known for a history of natural disturbance regimes that have been extensively described (Frelich 2002). The continental climate is characterized by brief summers (mean July temperature 19 °C), long, cold winters

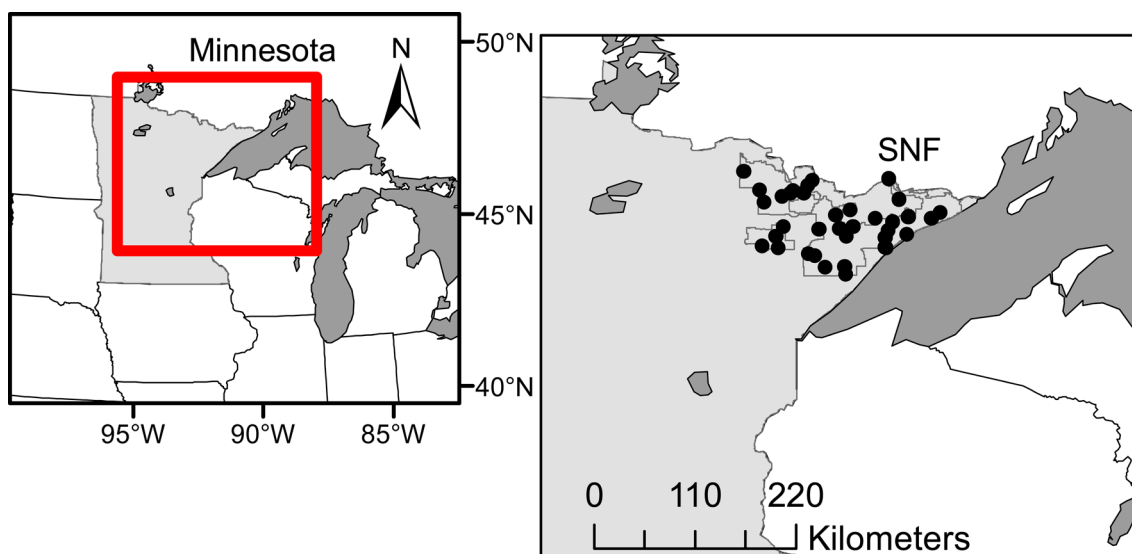


Fig. 1 Location of the Superior National Forest (*SNF*) and 36 forest stands in northern Minnesota, USA

(mean January temperature $-15\text{ }^{\circ}\text{C}$), and approximately 600–800 mm of annual precipitation. The presence of forest communities representative of two ecologically important biomes that are valued both for wood products and wilderness provides an ideal study area for deriving inferences relevant to broad areas of northern latitude forest.

Sampling design

Forest stands were selected and sampled in 2010 to represent the predominant forest communities occurring within the SNF and the broader Laurentian Mixed Forest Province of North America. Three 400-m² circular plots (spaced at least 28 m apart) were placed in stands of the most common forest types found in National Forest Inventory and Analysis data from 2004 to 2008. For the most abundant jack pine forest type, stands representative of both young and old stages of development were also sampled (Table 1), for a total of 108 plots in 36 forest stands. Within plots, overstory trees were mapped and measured for common structural attributes including diameter at breast height (DBH).

Dendrochronological analyses and live biomass estimation

Increment cores were extracted at 1.3 m from all live overstory trees (DBH > 10 cm) in each plot. Over 3,200 increment cores from 19 species were processed, measured using a Velmex measuring stage and cross-dated following standard dendrochronological techniques (Holmes 1983; Yamaguchi 1991). We reconstructed tree diameters from ring widths, DBH, and species-specific bark ratios (Dixon

and Keyser 2011), and calculated annual biomass increments at tree and stand scales (i.e., the mean of three plot totals) using species-specific allometric equations (Jenkins et al. 2004). We selected published allometric equations predicting whole tree biomass from DBH based on geographic proximity and DBH range (Online Resource 1). We defined the pith year at coring height to be the year of recruitment. For cores that missed the pith, a pith locator (Applequist 1958) was used to estimate the number of rings to the pith.

Simulating unobserved growth increments from stochastic mortality models

We simulated growth from non-surviving trees (“ghost trees”) that could not be observed in the live-tree sample starting in 2008 and working back through the dendrochronological record. This process consisted of repopulating the stand with trees whose growth or size structure at the time of mortality was defined by each of three mortality models. For all simulations, the annual mortality rate, or number of stems that died, was drawn each year from a uniform random distribution between 0 and 2 %, consistent with empirically measured annual mortality rates, which average 1 % and typically fall between 0 and 2 % for forests in the eastern US (Runkle 1985; Lorimer et al. 2001; Lines et al. 2010; Vanderwel et al. 2013). We estimated biomass increments for ghost trees by randomly drawing from the population of live trees and weighting the random draws according to three mortality models: mortality is random with respect to growth or tree size (M_0), mortality increases as tree biomass increment

Table 1 Forest types, species composition and structural characteristics sampled in 2010

Forest type	Code ^a	Dominant species (order of importance)	Stand age range 2008 (years) ^b	Mean basal area 2010 (m ² ha ⁻¹)	Mean density 2010 (trees ha ⁻¹)	Mean biomass 2010 (Mg ha ⁻¹)
Red/white pine	R/WP (1–3)	<i>Pinus resinosa</i> , <i>Pinus strobus</i> , <i>Betula papyrifera</i>	156–224	37.0	294	144.5
White/red pine	W/RP (4–6)	<i>Pinus strobus</i> , <i>Abies balsamea</i> , <i>Picea mariana</i>	71–109	35.9	564	122.8
Jack pine young	JP (1–3)	<i>Pinus banksiana</i> , <i>Picea mariana</i> , <i>Pinus resinosa</i>	31–47	25.6	1072	96.2
Jack pine old	JP (4–6)	<i>Pinus banksiana</i> , <i>B. papyrifera</i> , <i>Picea mariana</i>	62–87	27.2	794	114.3
Spruce/fir	S/F (1–3)	<i>A. balsamea</i> , <i>Populus tremuloides</i> , <i>Picea glauca</i>	37–71	24.3	858	97.8
Lowland conifer	WC (1–3)	<i>Thuja occidentalis</i> , <i>P. mariana</i> , <i>A. balsamea</i>	110–162	45.0	797	121.5
Lowland conifer	BS (4–6)	<i>P. mariana</i> , <i>Larix laricina</i>	75–121	16.7	875	68.7
Upland hardwood	RO (1–3)	<i>Quercus rubra</i> , <i>Acer rubrum</i>	68–92	15.9	728	91.4
Lowland hardwood	BA (1–3)	<i>Fraxinus nigra</i> , <i>T. occidentalis</i> , <i>A. balsamea</i>	80–141	23.4	722	63.5
Northern hardwood	SM (1–3)	<i>Acer saccharum</i> , <i>Acer rubrum</i> , <i>Betula alleghaniensis</i>	69–108	29.4	761	261.9
Aspen/birch	AB (1–3)	<i>P. tremuloides</i> , <i>Populus grandidentata</i> , <i>B. papyrifera</i> , <i>A. rubrum</i>	60–84	28.8	719	149.4
Aspen/birch conifer	BA (4–6)	<i>B. papyrifera</i> , <i>P. tremuloides</i> , <i>P. glauca</i> , <i>A. balsamea</i>	40–87	22.9	828	99.2

^a Forest-type codes include *letters* for forest type and *unique number* for each sampled stand (range in parentheses)

^b Twenty-fifth percentile of estimated pith age distribution measured from cores sampled at diameter at breast height

decreases (growth-related mortality; M_1), and the mortality distribution is u-shaped with respect to tree size (size-dependent mortality; M_2) (Buchman et al. 1983; Lorimer et al. 2001; Fraver et al. 2008; Lines et al. 2010; Caspersen et al. 2011; Hurst et al. 2011; Holzwarth et al. 2012) (Fig. 2). We then added growth of the simulated ghost-trees to the population sum and tracked it throughout the simulation working back through time until the population of surviving trees fell below 20 for each stand (See Online Resource 2 for detailed example). On average, we tallied 90 surviving trees per stand in 2010 (range of 39–177 trees).

We approximated M_1 by weighting the probability of random draws from survivors with a declining beta distribution ($\alpha = 0.5$, $\beta = 2$) relative to current growth (Fig. 2a). This probability density function places a higher probability of mortality on trees with low relative growth, assumed to be a sign of stress or poor competitive status. We modeled M_2 using an empirical relationship between tree diameter and mortality rates reported for *Acer saccharum* growing in similar Canadian forests (Caspersen et al. 2011) (Fig. 2b). We used this relationship because it fell in the middle of a range of species models (Caspersen et al. 2011; see Online Resource 2 for more details). For each year, we applied the randomly selected mortality rate (between 0 and 2 %) consistently across models, so that resulting differences in biomass increment reflect differences in the type of trees presumed to have died (fast or slow growing, small or large) according to the tested probability density functions. We calculated mean simulated growth and 95 %

empirical confidence intervals (CIs) from 40 replicate simulations per mortality model and stand combination.

Calculation of net aboveground biomass increment

We used the results of the size-dependent mortality simulations (M_2), which produced growth that was intermediate between M_0 and M_1 , to calculate annual net aboveground biomass increments (Net AGBi) for comparison with previous research that defines aboveground biomass increments as the balance between live wood production (Live AGBi) and the annual transfer of dead tree biomass from the live to dead wood pools.

$$\text{NetAGBi} = \sum_1^{\text{livetrees}} \text{AGBi} - \sum_1^{\text{deadtrees}} \text{AGB} \quad (1)$$

This balance reflects the concepts of forest yield and of net aboveground biomass change that is expected to approach zero under a paradigm of succession to a steady state (Bormann and Likens 1979). We calculated the median and 95 % CIs of Net AGBi and compared metrics of biomass development patterns with those calculated from Live AGBis alone.

Deriving mean trends in biomass increment from fitted splines

We estimated mean patterns of stand growth by fitting smoothing splines (Cook and Peters 1981) to the aggregate

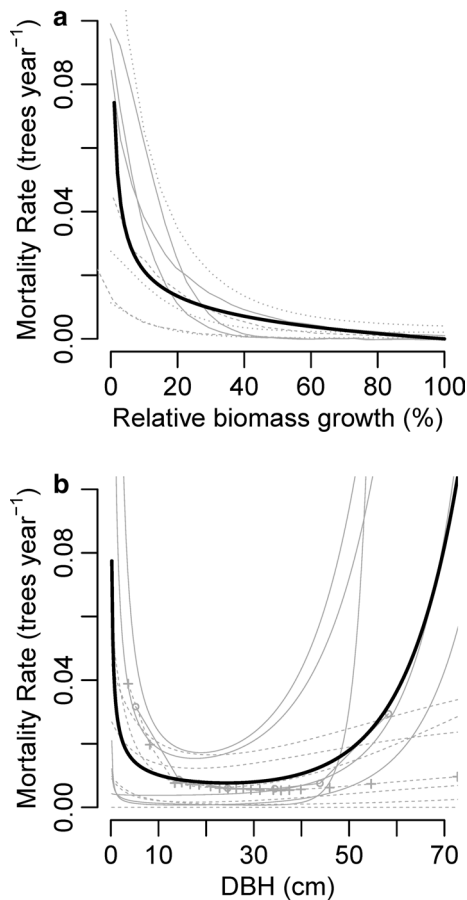


Fig. 2 Annual mortality models that assume mortality declines as relative growth increases (**a**) (growth-related mortality; M_1), or that mortality rates are u-shaped with respect to diameter at breast height (DBH) (**b**) (size-dependent mortality; M_2). We show that these models (black lines) are reasonable approximations of relationships (grey lines) published for growth by Buchman et al. (1983) (dotted lines for trees of average DBH), Pacala et al. (1993) (solid lines) and Hurst et al. (2011) (dashed lines) or for DBH published by Caspersen et al. (2011) (solid lines, circles) and Lines et al. (2010) (dashed lines, crosses). Symbols in **b** show mean of species' response

biomass increment of the surviving (sampled), and the repopulated (sampled and simulated) populations, for all mortality models. We compared splines and their trends to the general model of biomass change that assumes an early peak and subsequent decline in growth. Splines smooth out high-frequency variability in growth caused by inter-annual changes in weather, herbivory, reproduction and disturbance, while maintaining trends associated with stand development that are of interest here. We fit splines to stand-level aggregate Live AGBi using the *dpLR* package in R with a rigidity of 20 years to allow identification of peaks in biomass development for stands as young as 30 years of age (R Development Core Team 2011; Bunn 2008). We determined the first derivative of splines using the first difference approach and calculated metrics to summarize

trends in biomass development patterns. These metrics included the timing and magnitude of mean peak biomass and mean trends for set intervals before and after the peak, for each mortality model and for the observed sample of survivors alone (Table 2). As the concept of stand age has a tenuous definition for multicohort stands, we defined the 25th percentile of the pith year distribution as the approximate time of stand recruitment. This percentile captured early stand establishment and growth for both single and multicohort stands better than the median (Online Resource 3). We compared estimates of stand recruitment age calculated from all usable cores to ages calculated from only cores that included pith and found no significant difference.

Ordination and clustering of stand development patterns

To understand differences in the shapes of biomass increment patterns, we used the summary trend metrics (Table 2; Online Resource 4) as input for a nonmetric multidimensional scaling (NMDS) ordination (McCune and Grace 2002) in PC-ORD (McCune and Mefford 2011). NMDS uses a multivariate distance matrix among stands and iterates to a solution of ordination axes that minimize stress in the sample data space. We used a Euclidean distance matrix and the location of stands within ordination space to demonstrate among-stand similarities and differences in biomass increment development. As peak Live AGBi occurred in some stands either at the beginning or end of the time series, we chose to emphasize trends prior to peak biomass. This excluded one stand (R/WP 2) due to the ordination technique's intolerance of missing values. We constructed a secondary matrix from static observations of stand structure in 2010, including species importance value, density, basal area, height, biomass and stand age, which we used to generate an ordination biplot and interpret correlations with the NMDS axes. We applied Ward's agglomeration clustering algorithm to ordination axes scores to group forest stands by similar increment patterns (McCune and Grace 2002). We compared timing of peak growth to estimates of potential maximum cohort age by forest type as defined by Gustafson and Sturtevant (2013) (Table 3) using regression.

Results

Effects of mortality models on peak biomass estimates

Simulated tree populations produced temporal patterns of live biomass increment that often varied significantly among stands (Fig. 3; Online Resource 3). For most stands, 95 % CIs of Live AGBi overlapped among three mortality models in recent years, while some became more divergent as simulations extended into the past (e.g., Fig. 3b).

Table 2 Metrics summarizing trends in biomass increment patterns from fitted splines

Metric	Derivation	Units
Peak biomass increment (peak)	Maximum of fitted spline	Mg ha ⁻¹
Stand age at peak	Year (peak)—approximate year of stand recruitment	Years
Trend establishment to peak	Mean and SD of slope (recruitment year to peak year) ^a	Mg ha ⁻¹ year ⁻¹
Trend 20 years before peak	Mean and SD of slope 20 years pre-peak ^a	Mg ha ⁻¹ year ⁻¹
Trend 20 years after peak	Mean and SD of slope 20 years post-peak ^a	Mg ha ⁻¹ year ⁻¹
Trend 1978–2008	Mean and SD of slope 1978–2008 ^a	Mg ha ⁻¹ year ⁻¹

^a Slope refers to the first derivative of fitted splines. These trends were summarized for the size-dependent model (M_2) which produced biomass increment patterns and metrics intermediate between the other two mortality models

Table 3 Mean summary metrics and significant differences among biomass increment patterns derived from sampled tree population and populations simulated using three mortality models

Mortality model	Age at peak biomass (years) mean (SD)	Peak biomass increment (Mg ha ⁻¹) mean (SD)	Difference in peak biomass increment (from observed) (Mg ha ⁻¹)	Difference in peak biomass increment (from observed) (%) mean (SD)
Observed: survivors	76.51 (44.39) ^a	2.16 (1.04)	–	–
M_0 : random	47.17 (39.87) ^b	2.82 (1.44)	0.665 (0.562) ^a	30.9 (23.7) ^a
M_1 : growth-related	67.74 (46.25) ^a	2.34 (1.16)	0.181 (0.200) ^b	7.7 (7.35) ^b
M_2 : size-dependent	57.06 (40.53) ^{a,b}	2.71 (1.43)	0.554 (0.532) ^a	24.9 (18.3) ^a

Letters superscripts that differ indicate that means are significantly different according to Fisher's least significant difference multiple comparisons test with comparison-wise error rate of 0.05. Lack of different letters indicates that ANOVA F -test showed no significant difference among models

Variation in patterns among models was not consistent, as simulations were dependent on the distribution of sampled biomass increments and reconstructed DBH distributions, which varied by stand and over the course of stand development (Online Resource 3). The timing and magnitude of peak biomass growth often varied within stands among the three mortality models and the surviving population alone (Fig. 3). On average, random mortality (M_0) caused peak biomass increment to occur at an earlier age (47 years) than growth-related (M_1) mortality (67 years) or the observed population (77 years) (Table 3). Timing of peak growth was intermediate (57 years) and not significantly different from the other models when mortality was size dependent (M_2). We observed a significant positive relationship between timing of peak growth and maximum potential cohort age by forest type ($\beta = 0.28$, $r^2 = 0.21$, under M_2), meaning that the peak occurred near 30 % of potential stand age on average.

The mean peak biomass increment and thus productivity varied substantially among forest types and did not differ among mortality models (Table 3). However, peak Live AGBi from repopulated stands did differ from that of the surviving population alone (Table 3). On average, peak growth under M_0 and M_2 was significantly higher than survivor peak biomass increment (0.665 and 0.553 Mg ha⁻¹ higher, respectively), and growth under M_1 (0.181 Mg ha⁻¹ higher). These differences equate to 25–30 % larger estimates of peak growth relative to that observed from surviving trees alone. The timing and magnitude of peak growth

derived from median Net AGBi did not differ significantly from Live AGBi patterns under M_2 ($P = 0.75$ and $P = 0.54$, respectively). However, 95 % CIs of simulated dead and Net AGBis were large and increased with stand age as the potential for death of relatively large trees increased (Online Resource 3).

Discrimination of distinct biomass increment patterns

NMDS ordination of biomass increment trend metrics resulted in a two-dimensional solution that explained 98.1 % of the variance in the stand by trend distance matrix (axis 1 = 93.7 %, axis 2 = 4.4 %). Trend metrics all correlated significantly with the first axis (Online Resource 5). Peak biomass increment declined with increasing axis 1 scores (Kendall's τ of -0.572 to -0.701) as did pre-peak biomass increment trends and their SDs ($\tau = -0.690$ to -0.868). The age at peak biomass increased with axis 1 scores ($\tau = 0.483$ – 0.716). Peak biomass increment decreased with the number of years it took to reach the peak (log-linear regression $r^2 = 0.17$). Axis 2 was most strongly correlated (positively) with survivor peak biomass increment, and with the SD in the trend from 1978 to 2008.

Static forest structure characteristics from the secondary matrix correlated significantly ($\tau > 0.2$, $P \leq 0.05$) with the NMDS axes; stand age and height were positively correlated with axis 1, while stand density and importance values of *P. banksiana* were negatively correlated (Fig. 4a). Stand biomass, basal area, and importance values of *A.*

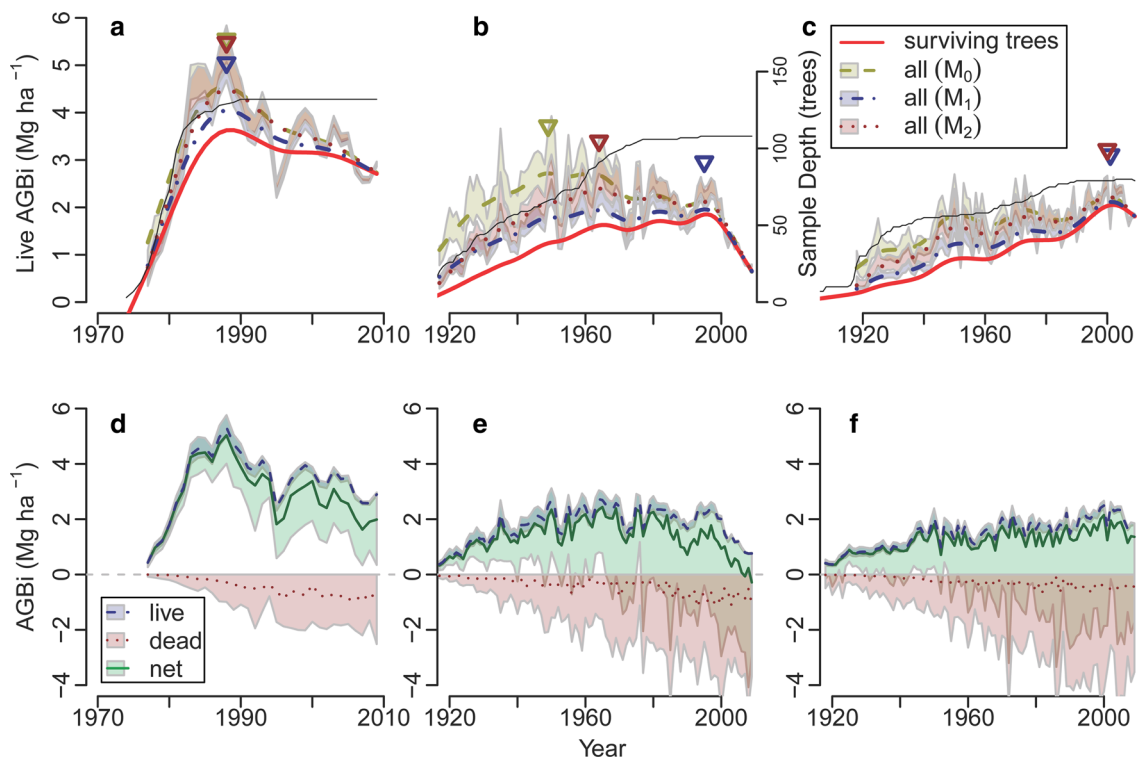


Fig. 3 Example biomass increment trends from surviving trees and three mortality model simulations (survivors + simulated trees) for a single stand from each of three forest types: **a, d** even-aged *Pinus banksiana*, **b, e** multi-cohort *Betula papyrifera* and *Abies balsamea*, and **c, f** multi-cohort *Quercus rubra*. Splines fit to mean growth (**bold lines**) highlight low frequency trends (**a–c**). Sample depth over time is shown by **thin black line**. Semi-transparent areas show 95 % con-

fidence intervals. **Triangles (a–c)** represent the year of peak growth and the quantity (offset by +1 Mg ha⁻¹ for clarity). Mortality models: random (M_0), growth-related (M_1), size-dependent (M_2). Net aboveground biomass increments (AGBi) (**d–f**) for the same stands using model M_2 shows that uncertainty in annual net AGBi is large, but median patterns (**solid green lines**) diverge little from live wood production (**Live AGBi; dashed blue lines**) (color figure online)

saccharum were positively correlated with axis 2. The strength and direction of these correlations illustrate potential drivers of the variation in biomass development patterns described below.

Statistical clustering in NMDS ordination space identified groups of stands with similar biomass development patterns (Fig. 4a) that were more diverse than expected (Fig. 4b–d). We observed the fastest growth and earliest peaks in young, even-aged *P. banksiana* forests (Fig. 4b), which agreed most closely with the early peak model. Forests that peaked slightly later ranged from an early peak to a parabolic shape for an *A. saccharum* stand, which may indicate forest decline (Fig. 4b; Online Resources 3, 4). Stands of intermediate productivity dominated by *Acer saccharum*, *Populus tremuloides*, or *Abies balsamea* grew fast prior to peak, after which Live AGBi tended to flatten (Fig. 4c). Forest stands with increasing positive scores on axis 1 (clusters 4–6) shifted from the peaked growth pattern to slow and continual increases in Live AGBi over stand development periods of up to 150 years (Fig. 4d). These low productivity stands (peak Live AGBi \sim 2 Mg ha⁻¹), often characterized by thin or vernal saturated soils, were

generally older and dominated by a range of species including *Quercus rubra*, *Fraxinus nigra*, *Thuja occidentalis*, or *Pinus resinosa*.

The trend in biomass increment 20 years after the peak was strongly and negatively related to the trend 20 years prior to the peak ($\beta = -0.22$, $r^2 = 0.78$). This indicates that growth declined at a proportional rate shortly after peaking. The recent trend (1978–2008) in Live AGBi across all stands was negative (mean -0.047 Mg ha⁻¹ year⁻¹, $P = 0.006$) and peak biomass growth was positively related to total stand biomass measured in 2010 ($\beta = 0.02$, $r^2 = 0.65$, M_2).

Discussion

Importance of past ghost-tree growth and mortality assumptions

Our study reconstructed aggregate growth of live trees, correcting for the biomass increment of ghost trees that died over the observation interval. Three mortality probability

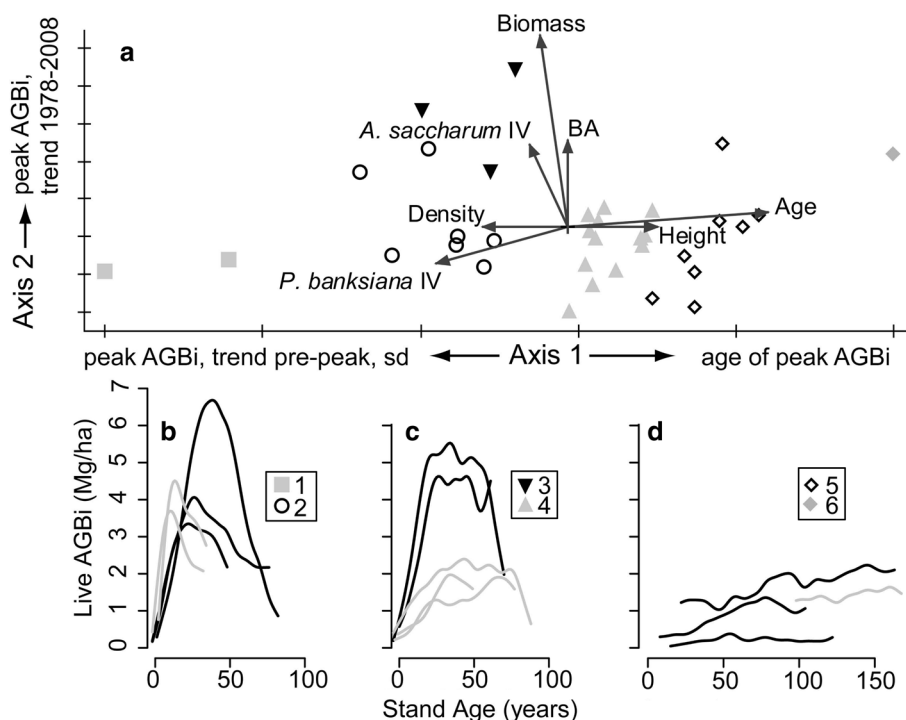


Fig. 4 Biplot of nonmetric multidimensional scaling (NMDS) ordination **a** of forest stands with respect to variation in biomass increment trends (Table 2). *Symbols* indicate membership in six statistically similar clusters. *Dark grey arrows* show direction and relative strength of significant correlations ($\tau > 0.200$) between static stand structural attributes measured in 2010 (secondary matrix) and NMDS axes. See Table 1 and Online Resources 3 and 4 for stand details. Biomass increment patterns varied among six clusters as shown by

representative stands (**b–d**). *Symbols* belong to the numbered statistical cluster indicated by the legend: **b** clusters 1–2 are characterized by rapid increases in Live AGBi and subsequent declines in growth; **c** clusters 3–4 contain stands that either plateau following fast early growth, or grow more slowly with lower peak AGBi; **d** remaining stands have lower maximum growth and flat or increasing Live AGBi trends that peak much later in stand development

distributions resulted in different estimates of the timing and magnitude of peak growth, with important implications for models of forest and ecosystem dynamics. When mortality was biased towards slow-growing individuals, reconstructed growth was lowest and differed least from the surviving sample. Random mortality best approximated past increments for old multi-cohort stands, because it better reflected early cohort growth when sample sizes were small (e.g., Online Resource 3; stands W/RP5, JP6). Size-dependent mortality yielded an unexpected emergent property in that the types of trees dying changed from smaller, and likely slow-growing trees, to larger trees over the course of stand development (Fig. 2). This temporal change in mortality was driven by the evolution of the underlying diameter distributions; growth under size-dependent mortality was most similar to growth-related simulations during early stand development when mean DBH was smaller than 15 cm, but became more similar to random simulations as diameters increased from 15 to 35 cm (Fig. 2b). This finding is consistent with recent research showing different modes of mortality across size classes (Holzwarth et al. 2012). Because few of our mature stand diameter

distributions exceeded 50-cm DBH, the full range of the u-shaped, size-dependent mortality function was rarely expressed. As trees in these forests grow to larger size classes and become more susceptible to size-related mortality, we would expect growth reconstructed under size-dependent mortality to exceed estimates from random or growth-related models. These simulations demonstrate how different mortality models affect reconstructions and projections of forest biomass growth and highlight the need to account for past mortality when estimating past growth from surviving trees.

Age-related decline not always observed in live biomass increment

Our reconstruction of past live tree biomass increments for eight forest communities often produced growth patterns that agreed with the early peak growth model, but also produced an array of divergent patterns (Fig. 3; Online Resources 3, 4). Patterns of live biomass increment generally tracked differences in species composition and age-structure, as illustrated by Fig. 4. Live AGBi peaked early

and declined most closely to the assumed model in stands that were monospecific, or nearly so, dense and even-aged (e.g., *Pinus banksiana* JP1-3 and 5, *Picea mariana* BS6, *A. saccharum* SM2 and 3). These patterns are reminiscent of data that informed Odum's (1969) hypothesis on age-related decline in forest productivity, which relied on a chronosequence of dense and pure *Abies sachalinensis* stands and a conceptual diagram reported by Kira and Shidei (1967). In contrast, other stands had Live AGBi patterns that were hump-shaped, which may indicate forests experiencing demographic transitions where initial cohorts of intolerant species experience mortality and release growing space that is captured by younger shade-tolerant species. Ingrowth of more shade-tolerant cohorts may compensate for growth lost to mortality, maintaining overall stand growth at a consistent level, or increasing productivity if subsequent dominant species grow to a larger stature (Wirth 2009). Many of the older, lower-productivity stands, including those dominated by *Q. rubra*, *T. occidentalis*, and *F. nigra*, showed evidence of peaking later in stand development, and may keep increasing until a disturbance or other process significantly alters the composition and structure. Positive growth trends in these stands suggest that age-related growth declines are not inevitable. Declines may be symptomatic primarily of even-aged forests composed of similar competitors, and less characteristic of growth in multi-aged, diverse natural forests that cover much of the landscape.

The causes of the early peak decline pattern are still debated, with greater weight attributed either to physiological or stand structural hypotheses relevant to declines in live biomass growth, or to demographic hypotheses related to changes in aboveground biomass balance resulting from mortality. Live tree biomass increment follows the age-related decline pattern in some systems (Binkley et al. 2002; Ryan et al. 2004; Goulden et al. 2011), inspiring explanations of the phenomenon from tree-level physiological constraints including nutrient limitation, hydraulic resistance, changes in allocation (Ryan et al. 2004; Genet et al. 2009), or stand-structural changes attributed to variation in competitive efficiency among dominant and suppressed trees (Smith and Long 2001; Coomes et al. 2012; Xu et al. 2012). The data informing most of these hypotheses arose from simple, even-aged forest types that establish after stand-replacing disturbance [*Nothofagus solandri* (Coomes et al. 2012)], or grow as single cohorts in plantation settings [*Eucalyptus saligna* (Binkley et al. 2002; Ryan et al. 2004)]. Similarly, the only species in our data whose importance values correlated significantly with the early peak pattern was *P. banksiana*, a fire-adapted, shade-intolerant pine generally known for even-aged, post-disturbance establishment. While our analysis does not address why declines may occur, the fact that the pattern was

evident in live biomass increments of some stands suggests that growth- or structure-related explanations are needed (Ryan et al. 2004). Dense, young stands of trees with similar competitive traits followed the early peak pattern in our data. The relative youth (and below-average height) of these stands precludes explanations attributing declines to tree-level physiological limitations or increasing hydraulic path length. Instead, we suggest that similar competitors in even-aged stands must compete for a limited layer of growing space, and thus changes in or a lack of variation in competitive efficiency offer a stronger explanation.

Other studies focused on the balance between growth and mortality often find that declines in Net AGBi are determined more by population or demographic processes (mortality) than by changes in tree growth (Acker et al. 2002; Taylor and MacLean 2005; Coomes et al. 2012; Xu et al. 2012). Our finding of protracted increasing growth in low-productivity stands conflicts with age-related physiological explanations because there is no evidence of decline. Rather, these patterns are more consistent with hypotheses attributing peaks in Net AGBi to mortality processes (Coomes et al. 2012; Xu et al. 2012), demonstrating that our data support multiple hypotheses. There is growing acceptance for the view that these hypotheses are not mutually exclusive, along with renewed interest in using empirical data to identify if, when, where, and why age-related declines occur (Lichstein et al. 2009; Wirth 2009). Our results suggest a need for new hypotheses to explain why growth may increase with stand age in some forests.

Models of expected stand biomass growth feed directly into analyses that seek to uncover trends associated with global change, including potential responses to increasing temperatures, growing season length or CO₂ concentrations. Our analysis demonstrates that without estimating past growth of ghost trees, many forests would show increasing trends in growth that could be interpreted (incorrectly) as evidence of CO₂ fertilization or response to some other changing environmental factor. Similarly, failure to incorporate the contribution of these ghost trees could undermine the accuracy of reconstructed negative climate change impacts on forest growth, notably increasing aridity in dryland regions (Hartmann 2011). Expecting aggregate stand growth to follow an idealized pattern that includes decline and interpreting departures from this expectation as evidence that growth has changed can lead to erroneous inferences about responses to global change, particularly when demographic processes such as past growth and mortality have not been correctly represented. Though we found a range of biomass patterns across forest types and ages, the mean trend from 1978 to 2008 was slightly negative, suggesting that it would be difficult to identify a positive response to recent climatic changes in these forests.

Model caveats and implications for dendrochronology

Our approach to estimate past growth from census tree-ring data relied on assumptions that may not always apply. Our random mortality rate was constrained between 0 and 2 % of stand density, meaning that infrequent, large pulses of synchronized mortality were not simulated. While more complex stochastic mortality rates, or specific mortality events, could be applied if details of past disturbance events were available, the rates used here were consistent with empirical observations of background mortality attributed to self-thinning and gap dynamics in northern temperate forests (Lorimer et al. 2001; Lines et al. 2010). Higher mortality rates would likely accentuate model differences in reconstructed growth. We note that uncertainty around estimates of annual Net AGBi (Fig. 3) was large, compared to Live AGBi, because Net AGBi is dependent on the year in which individual large trees die, which is highly stochastic over 40 replicate simulations. Average or median rates of net growth across simulations were relatively stable over time, while predicting mortality in any specific year was highly uncertain. In addition, uncertainty in estimated growth increased as simulations extended further into the past. While we limited simulations to time periods with at least 20 surviving trees, we advise caution in interpreting the oldest curve patterns. Our approach of reconstructing biomass also required DBH and a representative sampling design (Brienen et al. 2012), characteristics not universally recorded in dendrochronology collections. Given the intense effort expended to core trees and analyze ring widths, tree ring databases would be significantly enhanced if DBH was consistently measured and reported with ring-width series.

Conclusion

Our analysis demonstrates that tree-ring reconstructions from naturally established forests provide a means to estimate long-term annual-resolution changes in Live AGBi. Estimates of the timing and magnitude of past growth peaks depend on accounting for past mortality. The resulting Live AGBi curves illustrate more diverse biomass development patterns than have emerged from repeat inventory, permanent sample plots or chronosequence studies of simplified, monospecific forests or assumed successional sequences. The fact that growth trends increased steadily for several forests highlights the importance of remeasuring these stands over time and suggests that age-related growth declines are neither inevitable nor characteristic of all forest types. Future monitoring can help determine if biomass is simply developing slowly, to eventually peak and decline, or whether biomass increment can increase until

a disturbance ends the biomass accumulation process. As steadily increasing biomass growth in low-productivity forests has not been reported previously, the evolution of these trends is of particular interest. Future research combining long-term plot remeasurement data with the approaches demonstrated here could help attribute growth and mortality responses to either environmental change or stand development. Our ability to detect growth responses to global change or to model future forest dynamics depends on how accurately we understand and recreate these patterns of biomass development.

Acknowledgments Funding for this research was provided by the American Revenue Recovery Act and the US Department of Interior Northeast Climate Science Center. Nick Jensen, Mike Reinikainen, John Segari, Kyle Gill, Amy Milo and others collected field data and/or measured and cross-dated tree rings. We thank Bruce Anderson and the Superior National Forest for logistical support and Shawn Fraver and two anonymous reviewers for reviewing this manuscript. Any use of trade, product, or firm names is for descriptive purposes only and does not imply endorsement by the U.S. Government.

References

- Acker SA, Halpern CB, Harmon ME, Dyrness CT (2002) Trends in bole biomass accumulation, net primary production and tree mortality in *Pseudotsuga menziesii* forests of contrasting age. *Tree Physiol* 22:213–217
- Applequist MB (1958) A simple pith locator for using with off-center increment cores. *J For* 56:141
- Binkley D, Stape JL, Ryan MG, Barnard HR, Fownes J (2002) Age-related decline in forest ecosystem growth: an individual-tree, stand-structure hypothesis. *Ecosystems* 5:58–67
- Bormann FH, Likens GE (1979) Catastrophic disturbance and the steady-state in Northern hardwood forests. *Am Sci* 67:660–669
- Bradford JB, Kastendick DN (2010) Age-related patterns of forest complexity and carbon storage in pine and aspen-birch ecosystems of northern Minnesota, USA. *Can J For Res* 40:401–409
- Brienen RJW, Gloor E, Zuidema PA (2012) Detecting evidence for CO₂ fertilization from tree ring studies: the potential role of sampling biases. *Glob Biogeochem Cycles* 26:GB1025
- Buchman RG, Pederson SP, Walters NR (1983) A tree survival model with application to species of the Great Lakes region. *Can J For Res* 13:601–608
- Bunn AG (2008) A dendrochronology program library in R (dplR). *Dendrochronologia* 26:115–124
- Caspersen JP, Pacala SW, Jenkins JC, Hurtt GC, Moorcroft PR, Birdsey RA (2000) Contributions of land-use history to carbon accumulation in US forests. *Science* 290:1148–1151
- Caspersen JP, Vanderwel MC, Cole WG, Purves DW (2011) How stand productivity results from size- and competition-dependent growth and mortality. *PLoS ONE* 6:e28660
- Clark DA, Brown S, Kicklighter DW, Chambers JQ, Thomlinson JR, Jian N (2001) Measuring net primary production in forests: concepts and field methods. *Ecol Appl* 11:356–370
- Clark JS, Wolosin M, Dietze M, Ibanez I, LaDeau S, Welsh M, Kloeppel B (2007) Tree growth inference and prediction from diameter censuses and ring widths. *Ecol Appl* 17:1942–1953
- Cole CT, Anderson JE, Lindroth RL, Waller DM (2010) Rising concentrations of atmospheric CO₂ have increased growth in natural

- stands of quaking aspen (*Populus tremuloides*). *Glob Change Biol* 16:2186–2197
- Cook ER, Peters K (1981) The smoothing spline: a new approach to standardizing forest interior tree-ring width series for dendroclimatic studies. *Tree-Ring Bull* 41:45–53
- Coomes DA, Holdaway RJ, Kobe RK, Lines ER, Allen RB (2012) A general integrative framework for modeling woody biomass production and carbon sequestration rates in forests. *J Ecol* 100:42–64
- Davis SC, Hessl AE, Scott CJ, Adams MB, Thomas RB (2009) Forest carbon sequestration changes in response to timber harvest. *For Ecol Manage* 258:2101–2109
- Dixon GE, Keyser CE (2011) Northeast (NE) variant overview forest vegetation simulator. U.S. Department of Agriculture, Forest Service, Forest Service Management Service Center, Fort Collins
- Duchesne L, Ouimet R, Morneau C (2003) Assessment of sugar maple health based on basal area growth pattern. *Can J For Res* 33:2074–2080
- Foster JR, Burton JI, Forrester JA, Liu F, Muss JD, Sabatini FM, Scheller RM, Mladenoff DJ (2010) Evidence for a recent increase in forest growth is questionable. *Proc Natl Acad Sci* 107:E86–E87
- Fraver S, Jonsson BG, Jönsson M, Esseen PA (2008) Demographics and disturbance history of a boreal old-growth *Picea abies* forest. *J Veg Sci* 19:789–798
- Frellich LE (2002) Forest dynamics and disturbance regimes studies from temperate evergreen-deciduous forests. Cambridge University Press, Cambridge
- Genet H, Breda N, Dufrene E (2009) Age-related variation in carbon allocation at tree and stand scales in beech (*Fagus sylvatica* L.) and sessile oak (*Quercus petraea* (Matt.) Liebl.) using a chronosequence approach. *Tree Physiol* 30:177–192
- Goulden ML, McMillan AMS, Winston GC, Rocha AV, Manies KL, Harden JW, Bond-Lamberty BP (2011) Patterns of NPP, GPP, respiration, and NEP during boreal forest succession. *Glob Change Biol* 17:855–871
- Gower ST, McMurtrie RE, Murty D (1996) Above-ground net primary production decline with stand age: potential causes. *Trends Ecol Evol Res* 11:378–382
- Gustafson EJ, Sturtevant BR (2013) Modeling forest mortality caused by drought stress: implications for climate change. *Ecosystems* 16:60–74
- Hartmann H (2011) Will a 385 million year-struggle for light become a struggle for water and for carbon? - How trees may cope with more frequent climate change-type drought events. *Glob Change Biol* 17:642–655
- Holmes RL (1983) Computer-assisted quality control in tree-ring dating and measurement. *Tree-Ring Bull* 43:69–78
- Holzwarth F, Kahl A, Bauhus J, Wirth C (2012) Many ways to die, partitioning tree mortality dynamics in a near-natural mixed deciduous forest. *J Ecol*. doi:10.1111/1365-2745.12015
- Hurst JM, Allen RB, Coomes DA, Duncan RP (2011) Size-specific tree mortality varies with neighborhood crowding and disturbance in a montane *Nothofagus* forest. *PLoS ONE* 6:e26670
- Jenkins JC, Chojnacky DC, Heath LS, Birdsey RA (2004) Comprehensive database of diameter-based biomass regressions for North American tree species. Gen Tech Rep NE-319. U.S. Department of Agriculture, Forest Service, Northeastern Research Station, Newtown Square
- Johnson SE, Abrams MD (2009) Age class, longevity and growth rate relationships: protracted growth increases in old trees in the eastern United States. *Tree Physiol* 29:1317–1328
- Johnson EA, Miyanishi K (2008) Testing the assumptions of chronosequences in succession. *Ecol Lett* 11:419–431
- Kira T, Shidei T (1967) Primary production and turnover of organic matter in different forest ecosystems of the Western Pacific. *Ecol Soc Jpn* 17:70–87
- Lichstein JW, Wirth C, Horn HS, Pacala SW (2009) Biomass chronosequences of United States forests: implications for carbon storage and forest management. In: Wirth C, Gleixner G, Heimann M (eds) Old-growth forests: function, fate and value. Ecological studies vol. 207. Springer, Berlin, pp 301–341
- Lines ER, Coomes DA, Purves DW (2010) Influences of forest structure, climate and species composition on tree mortality across the eastern US. *PLoS ONE* 5(10):e13212
- Lorimer CG, Dahir SE, Nordheim EV (2001) Tree mortality rates and longevity in mature and old-growth hemlock-hardwood forests. *J Ecol* 89:960–971
- Luyssaert S, Schulze-Detlef E, Börner A, Knohl A, Hessenmoller D, Law BE, Ciais P, Grace J (2008) Old-growth forests as global carbon sinks. *Nature* 455:213–215
- Malhi Y, Baker TR, Phillips OL, Almeida S, Alvarez E, Arroyo L, Chave J, Czimczik CI, Di Fiore A, Higuchi N, Killeen TJ, Laurance SG, Laurance WF, Lewis SL, Montoya LMM, Monteagudo A, Neill DA, Vargas PN, Patino S, Pitman NCA, Quesada CA, Salomao R, Silva JNM, Lezama AT, Martinez RV, Terborgh J, Vince B, Lloyd J (2004) The above-ground coarse wood productivity of 104 Neotropical forest plots. *Glob Change Biol* 10:563–591
- McCune B, Grace JB (2002) Analysis of ecological communities. MjM Software Design, Gleneden Beach
- McCune G, Mefford MJ (2011) PC-ORD. Multivariate analysis of ecological data. Version 6.0. MjM Software, Gleneden Beach
- Metsaranta JM, Lieffers VJ (2010) Patterns of inter-annual variation in the size asymmetry of growth in *Pinus banksiana*. *Oecologia* 163:737–745
- Odum E (1969) The strategy of ecosystem development. *Science* 164:262–270
- Pacala SW, Canham CD, Silander JA Jr (1993) Forest models defined by field measurements. I. The design of a northeastern forest simulator. *Can J For Res* 23:1980–1988
- Phipps RL, Whiton JC (1988) Decline in long-term growth trends of white oak. *Can J For Res* 18:24–32
- Pregitzer KS, Euskirchen ES (2004) Carbon cycling and storage in world forests: biome patterns related to forest age. *Glob Change Biol* 10:2052–2077
- R Development Core Team (2011) R: a language and environment for statistical computing. R Foundation for Statistical Computing, Vienna. ISBN 3-900051-07-0. URL <http://www.R-project.org/>
- Rhemtulla JM, Mladenoff DJ, Clayton MK (2009) Historical forest baselines reveal potential for continued carbon sequestration. *Proc Natl Acad Sci* 106:6082–6087
- Runkle JR (1985) Disturbance regimes in temperate forests. In: Pickett STA, White PS (eds) The ecology of natural disturbance and patch dynamics. Academic Press, San Diego, pp 17–33
- Ryan MG, Binkley D, Fownes JH (1997) Age-related decline in forest productivity: pattern and process. *Adv Ecol Res* 27:213–262
- Ryan MG, Binkley D, Fownes JH, Gardina CP, Senock RS (2004) An experimental test of the causes of forest growth decline with stand age. *Ecol Monogr* 74:393–414
- Smith FW, Long JN (2001) Age-related decline in forest growth: an emergent property. *For Ecol Manage* 144:175–181
- Taylor SL, MacLean DA (2005) Rate and causes of decline of mature and overmature balsam fir and spruce stands in New Brunswick, Canada. *Can J For Res* 35:2479–2490
- Vanderwel MC, Coomes DA, Purves DW (2013) Quantifying variation in forest disturbance and its effects on aboveground biomass dynamics, across the eastern United States. *Glob Change Biol* 19:1504–1517
- Williams AP, Allen CD, Miller CI, Swetnam TW, Michaelson J, Still CJ, Leavitt SW (2010) Forest responses to increasing aridity and warmth in the southwestern United States. *Proc Natl Acad Sci* 107:21289–21294

- Wirth C (2009) Old-growth forests: function, fate and value, a synthesis. In: Wirth C, Gleixner G, Heimann M (eds) Old-growth forests: function, fate and value. Ecological studies vol 207. Springer, Berlin, pp 465–491
- Xu C, Turnbull MH, Tissue DT, Lewis JD, Carson R, Schuster WSF, Whitehead D, Walcroft AS, Li J, Griffin KL (2012) Age-related decline of stand biomass accumulation is primarily due to mortality and not to reduction in NPP associated with individual tree physiology, tree growth or stand structure in a *Quercus*-dominated forest. *J Ecol* 100:428–440
- Yamaguchi DK (1991) A simple method for cross-dating increment cores from living trees. *Can J For Res* 21:414–416